



Title	Are males just passive? Coupling mechanism of the Brazilian cave insects with inverted genitalia
Author(s)	Cheng, Zixin; Kamimura, Yoshitaka; Ferreira, Rodrigo L. et al.
Citation	Science of nature, 110 https://doi.org/10.1007/s00114-023-01855-8
Issue Date	2023-06-01
Doc URL	https://hdl.handle.net/2115/92524
Rights	This version of the article has been accepted for publication, after peer review (when applicable) and is subject to Springer Nature' s AM terms of use, but is not the Version of Record and does not reflect post-acceptance improvements, or any corrections. The Version of Record is available online at: http://dx.doi.org/10.1007/s00114-023-01855-8
Type	journal article
File Information	2023_NAWI.pdf



1 **Are males just passive? Coupling mechanism of the Brazilian cave insects with**
2
3 **inverted genitalia**

4 Zixin Cheng^{1, 2}, Yoshitaka Kamimura³, Rodrigo L. Ferreira⁴, Charles Lienhard⁵ and
5 Kazunori Yoshizawa¹

6 ¹. Systematic Entomology, School of Agriculture, Hokkaido University, Sapporo 060-8589, Japan

7 ² State Key Laboratory of Freshwater Ecology and Biotechnology, Institute of Hydrobiology,
8 Chinese Academy of Sciences, Wuhan 430072, China

9 ³. Department of Biology, Keio University, Yokohama 223-8521, Japan

10 ⁴. Department of Ecology and Conservation, Federal University of Lavras, CEP 37200-900 Lavras
11 (MG), Brazil

12 ⁵. Geneva Natural History Museum, CP 6434, 1211 Geneva 6, Switzerland

13 Correspondances

14 Zixin Cheng

15 zixin@ihb.ac.cn

16 Kazunori Yoshizawa

17 psocid@agr.hokudai.ac.jp

18
19 **Abstract**

20 Species of the Brazilian cave barklouse genus *Neotrogla* (Psocodea: “Psocoptera”:

1 21 Trogiomorpha: Prionoglarididae: Sensitibillini) are known to have a “female penis
2
3 22 (gynosome)” that functions as an intromittent organ inserted into the membranous
4
5
6 23 pouches in the simple male genital chamber during copulation to receive semen.
7
8
9 24 However, the functions of other male and female genital structures and the copulatory
10
11 25 processes of *Neotroglia* were completely unknown to date. Based on μ CT observation
12
13
14 26 of the male and female postabdomen and connected muscles both before and in copula,
15
16
17 27 we clarified the functions of the male and female genital structures. In addition, based
18
19
20 28 on the analyses of the established 3D models, we concluded that precise and rigid
21
22
23 29 contact of multiple genital structures, and step-by-step releases of each holding
24
25
26 30 mechanism achieved by the cooperation of both sexes are involved in the copulatory
27
28
29 31 processes. The coevolution between the male and female genital structures in *Neotroglia*
30
31 32 may provide a new example for the evolution of tolerance traits.

33

34

35 **Keywords**

36 genitalia, copulatory processes, sexual selection, muscles

37

38

39

40

41

42

1
2
3
4
5
6
7
8
9
10
11
12
13
14
15
16
17
18
19
20
21
22
23
24
25
26
27
28
29
30
31
32
33
34
35
36
37
38
39
40
41
42
43
44
45
46
47
48
49
50
51
52
53
54
55
56
57
58
59
60
61
62
63
64
65

1 43 **Introduction**

2
3 44 The Brazilian cave insect genus *Neotrogla* (Psocodea: Trogiomorpha: Prionoglarididae:
4
5
6 45 Sensitibillini) has been receiving much attention since it was discovered that the
7
8
9 46 females have a penis-like intromittent structure called gynosome (Lienhard *et al.*, 2010).
10
11
12 47 The gynosome, generally known as a female penis, is inserted into a vagina-like male
13
14 48 structure during copulation to obtain semen (Yoshizawa *et al.*, 2014). The female penis
15
16
17 49 has also been found in the African genus *Afrotrogla* (Lienhard, 2007). Both *Neotrogla*
18
19
20 50 and *Afrotrogla* belong to the small tribe Sensitibillini, containing three genera and
21
22
23 51 eleven named species only, and the well-developed female penis is considered to have
24
25
26 52 evolved independently in these two genera (Yoshizawa *et al.*, 2018b; Cheng *et al.*, 2023).
27
28 53 In recent years, several in-depth studies have been conducted on the factors affecting
29
30
31 54 the formation of female intromittent structures, such as the oligotrophic environment,
32
33
34 55 male nuptial gifts, female multiple sperm storage, female-above copulating position,
35
36
37 56 elongated spermathecal duct, and the absence of male penetrative genitalia (Yoshizawa
38
39 57 *et al.*, 2014, 2018ab, 2019; Kamimura *et al.*, 2021).

40
41
42 58 All these studies focused on the intromittent female penis, but the morphology and
43
44
45 59 function of other genital structures in these sex-reversed insects are still poorly
46
47
48 60 understood. Referring to muscle homology, Cheng *et al.* (2023) determined that the
49
50
51 61 female penis evolved from the spermapore plate, and its unique intromittent function is
52
53
54 62 brought by two pairs of novel muscles formed only within the Sensitibillini. Are there
55
56
57 63 novel structures and muscles in the other genital structures? What functions do other
58
59 64 genital structures have during copulation? Do females copulate coercively, and are
60
61
62
63
64
65

1 65 males just passive for mating? What types of sexual selection are strongly reflected in
2
3 66 the copulatory processes? All these questions need to be answered under the overall
4
5
6 67 grasp of the structures of male and female genitalia and the copulatory processes of
7
8
9 68 these cave insects with inverted genitalia.

10
11 69 In this study, by using the synchrotron μ CT technique, we present 3D models of
12
13
14 70 the whole male and female genital structures and their associated muscles of *Neotrogl*
15
16
17 71 *curvata*. By comparing the morphological changes of the genital structures and
18
19
20 72 associated muscles before and during copulation, we clarify the functions of these
21
22
23 73 structures and estimate the complete copulatory processes. We also analysed the
24
25
26 74 homology of the muscles between *Neotrogl*a species and the other non-genital-reversed
27
28 75 Psocodea and traced the origin of each structure and muscle of *Neotrogl*a.

29
30
31 76

32 33 34 77 **Materials and Methods**

35
36 78 A copulating pair and a noncopulating male and female of the coupling-role reversed
37
38
39 79 cave psocid *Neotrogl*a *curvata* Lienhard & Ferreira, 2013 (Trogiomorpha) were
40
41
42 80 examined. A noncopulating male and female of *N. brasiliensis* Lienhard, 2010
43
44
45 81 (Lienhard et al., 2010) and noncopulating male specimens of *Trichadenotecnum*
46
47
48 82 *pseudomedium* Yoshizawa, 2001 (Psocomorpha: Cheng & Yoshizawa, 2019), the latter
49
50
51 83 of which has normal genital structures, were also examined for comparison. All samples
52
53
54 84 were subjected to μ CT examination, and voucher specimens were stored in the
55
56
57 85 Hokkaido University Insect Collection. Samples were fixed either with hot water, FAA
58
59
60 86 solution (formalin:alcohol:acetic acid = 6:16:1), or 80% ethanol and then preserved in

1 87 80% ethanol. Dehydration was conducted in ascending order with 80–100% ethanol
2
3 88 before drying them at the critical point (EM CPD300, Leica, Wetzlar, Germany) to
4
5
6 89 remove water without serious organ shrinkage. Samples were then scanned by
7
8
9 90 synchrotron μ CT at the BL47XU (Uesugi et al., 2012) beamline of the Super Photon
10
11 91 ring-8 GeV (SPring-8; Hyogo, Japan) using a stable beam energy of 8 keV in
12
13
14 92 absorption-contrast mode. The tomography system consists of a full-field X-ray
15
16
17 93 microscope with Fresnel zone plate optics (Uesugi et al., 2017). We used semiautomatic
18
19
20 94 segmentation algorithms based on grey-value differences in ITK-SNAP software
21
22
23 95 (Yushkevich et al., 2006) to obtain 3D representations of the terminalia of all three
24
25
26 96 species.

27
28 97

30 98 **Results**

31
32
33 99 We first describe the muscles associated with male and female terminalia of *Neotrogla*
34
35
36 100 *curvata*. We grouped the muscles according to their origin as follows: muscles of the
37
38
39 101 epiproct [ep]; paraproct [pa]; subgenital plate [sg]; dorsal valve [do]; external valve
40
41
42 102 [ex]; spermapore plate/gynosome or the membrane surrounding it [sp/gy]; hypandrium
43
44
45 103 [hy]; and phallosome [ph].

46
47
48
49 104 Abbreviations: O – origin; I – insertion; and F – assumed function based on
50
51
52 105 morphological conditions.

53
54
55
56 106 **epX01** (male/female) (Figs. 2C, D and 8A: = 01 of Cheng & Yoshizawa, 2019); O:
57
58
59 107 mid-dorsal site of clunium (segment IX); I: posterior end of the epiproct; and F: closure

1 108 and/or flipping of the epiproct.
2
3
4
5 109 **paX01** (male/female) (Figs. 2C, D and 8A: = 02 of Cheng & Yoshizawa, 2019); O:
6
7 110 anterolateral region of the clunium (segment X); I: anterodorsal end of the paraproct,
8
9 111 very close to the posterolateral margin of the epiproct; and F: involved in opening the
10
11 112 paraproct.
12
13
14
15
16
17 113 **paX02** (male/female) (Figs. 2C, D and 8A: = 02 of Cheng & Yoshizawa, 2019); O:
18
19 114 mediodorsal region of the clunium (segment X); I: anterodorsal end of the paraproct,
20
21 115 very close to the anterolateral corner of the epiproct; and F: involved in opening the
22
23 116 paraproct.
24
25
26
27
28
29 117 **paX03** (male/female) (Figs. 2C, D and 8A: = 03 of Cheng & Yoshizawa, 2019); O:
30
31 118 mediolateral region of the clunium (segment X); I: internal margin of the paraproct near
32
33 119 the anal opening; and F: involved in retracting the paraproct.
34
35
36
37
38
39 120 **paX04** (male/female) (Figs. 2C, D and 8A); O: mediolateral region of the clunium
40
41 121 (segment IX); I: anterolateral margin of the paraproct; and F: involved in retracting the
42
43 122 paraproct.
44
45
46
47
48
49 123 **dosp01** (female) (Figs. 2E, F and 8A: = 05 of Cheng & Yoshizawa, 2019); O: base of
50
51 124 the dorsal valve; I: on the membrane connected to the spermapore plate/gynosome, near
52
53 125 the posterior tip of the spermapore plate; and F: involved in restoring the position of
54
55 126 the gynosome (spermapore plate) and the dorsal valve.
56
57
58
59 127 **doex01** (female) (Figs. 2E, F and 8A); O: base of the dorsal valve; I: base of the external
60
61
62
63
64
65

1 128 valve; and F: involved in restoring the position of the dorsal valve and closure of the
2
3
4 129 external valve.
5
6 130 **exsp01** (female) (Figs. 2E, F and 8A: = 06 of Cheng & Yoshizawa, 2019); O: base of
7
8
9 131 the external valve; I: on the membrane connected to the spermapore plate/gynosome,
10
11 132 near the posterior tip of the spermapore plate; and F: involved in restoring the position
12
13 133 of the gynosome (spermapore plate) and closure of the external valve.
14
15
16 134 **exIX02** (female) (Figs. 2E, F and 8A: = 08 of Cheng & Yoshizawa, 2019); O:
17
18
19 135 anterolateral margin of the clunium; I: base of the external valve, near the middle of the
20
21 136 junction with the clunium; and F: involved in opening the external valve.
22
23
24 137 **exVIII01** (female) (Figs. 2E, F and 8A); O: medioventral region of sternum VIII; I:
25
26
27 138 base of the external valve; and F: involved in closure of the external valve.
28
29
30 139 **spIX01** (female) (Figs. 2G, H and 8A); O: mediolateral region of the clunium; I: on the
31
32
33 140 spermapore membrane; and F: involved in restoring the gynosomal spiny membrane
34
35 141 (*Neotroglia*) or the position of the spermapore plate (other Psocodea).
36
37
38 142 **spIX02** (female) (Figs. 2G, H and 8A); O: mediolateral region of the clunium; I: on
39
40
41 143 the spermapore membrane; and F: involved in restoring the gynosomal spiny
42
43 144 membrane (*Neotroglia*) or the position of the spermapore plate (other Psocodea).
44
45
46 145 **gyIX01** (female) (Figs. 2G, H and 8A); O: gynosome membrane very close to dorsal
47
48
49 146 valves (=ventral membrane of segment IX); I: anterior end of the basal shaft; and F:
50
51 147 protractors of the gynosome.
52
53
54 148 **gy-01** (female) (Figs. 2G, H and 8A); O: an internal organ (specific insertion site not
55
56
57 149 detected); I: anterior end of the basal shaft; and F: retractors of the gynosome.
58
59
60
61
62
63
64
65

1 150 **papa01** (male) (Figs. 5C, D and 8B); O: internal margin of the paraproct near the anal
2
3 151 opening; I: anterolateral margin of the paraproct; and F: involved in opening the anus.

4
5
6 152 **pahy01** (male) (Figs. 3F, 5C, D and 8B: = 04 of Cheng & Yoshizawa, 2019); O:
7
8 153 anteroventral end of the paraproct; I: anterolateral region of the hypandrium (segment
9
10 154 IX); and F: involved in indirectly opening the hypandrium and retracting the male
11
12 155 paraproct (holding the female dorsal valve during copulation: see below).

13
14
15
16
17 156 **hyVIII01** (male) (Figs. 3F, 5E, F and 8B: = 05 of Cheng & Yoshizawa, 2019); O:
18
19 157 posterolateral region of segment VIII; I: mediolateral margin of the hypandrium; and F:
20
21 158 involved in restoring the hypandrium.

22
23
24
25 159 **phIX01** (male) (Figs. 3F-I, 5G, H and 8B: = 07 of Cheng & Yoshizawa, 2019); O: U-
26
27 160 shaped end of the sclerite of the phallosome; I: anterolateral region of the hypandrium
28
29 161 (segment IX); and F: involved in opening the hypandrium/protrusion of the phallosome.

30
31
32
33 162 **phIX02** (male) (Figs. 3F-I, 5G, H and 8B: = 08 of Cheng & Yoshizawa, 2019); O:
34
35 163 middle of the sclerite of the phallosome; I: anterolateral region of the hypandrium
36
37 164 (segment IX), phIX01, phIX02 and the sclerite of the phallosome present a triangle in
38
39 165 position; and F: involved in opening the hypandrium/retraction of the phallosome.

40
41
42
43
44 166 **phVIII01** (male) (Figs. 3F-I, 5G, H and 8B); O: posterolateral region of segment VIII;
45
46 167 I: posterior of the sclerite of the phallosome; and F: involved in protrusion of the
47
48 168 phallosome (holding the female dorsal valve during copulation: see below).

49
50
51
52
53 169

54 55 56 57 170 **Skeletal and muscle structures of female terminalia**

58
59 171 Among the female terminal structures of *Neotroglia*, the morphology of the clunium and
60
61
62
63
64
65

1 172 the epiproct is not much different from those of the other females of Psocodea. In
2
3 173 contrast, the subgenital plate (posterior extension of the 8th sternum) is completely
4
5
6 174 reduced in *Neotroglia*. A distinct difference was also detected in the paraproct between
7
8
9 175 *Neotroglia* and other psocodeans, i.e., two concavities are present on the ventrolateral
10
11
12 176 surface of the paraproct in *Neotroglia* (Fig. 1B). One group of muscles (epX01; Fig. 2C)
13
14 177 is associated with the epiproct, and four groups of muscles (paX01-04; Fig. 2C) with
15
16
17 178 the paraproct, all of which originate from the clunium. All of these muscles are
18
19
20 179 homologous to those associated with the epiproct or paraproct of other psocodeans
21
22
23 180 (Cheng & Yoshizawa, 2022).

24
25 181 The bases of the external valve of the gonapophyses are connected by a transverse
26
27
28 182 sclerite (Fig. 3B). The dorsal valve of the gonapophyses is located posteromedially to
29
30
31 183 the transverse sclerite of the external valves and forms an independent structure (Fig.
32
33
34 184 1A). The dorsal valve is not truly a paired structure like the external valves. It is usually
35
36
37 185 paired in Psocodea, but forms a single lobe-like structure with a posterior and lateral
38
39 186 marginal ridge shaped like a chair with a central depression (Fig. 3A). Two groups of
40
41
42 187 muscles (dosp01 and doex01; Fig. 2E) are connected to the dorsal valve. They are
43
44
45 188 homologous with those associated with the dorsal valves of other psocodeans (Cheng
46
47
48 189 & Yoshizawa, 2022).

49
50 190 The external valves form a pair of projections, together forming a crab claw-like
51
52
53 191 structure, basally connected by a transverse sclerite. The transverse sclerite is laterally
54
55
56 192 articulated with the clunium and anteriorly connected with sternum VIII (Fig. 1A, C).
57
58
59 193 The external valves of both *Neotroglia* species show a similar morphology (Fig. 3C).
60
61
62
63
64
65

1 194 There are four groups of muscles (doex01, exsp01, exIX02, exVIII01; Fig. 2E)
2
3 195 connected to the external valve, and three groups of those muscles are homologous with
4
5
6 196 those associated with the external valves of other psocodeans (Fig. 2E and 8A; Cheng
7
8
9 197 & Yoshizawa, 2022). The exVIII01 muscle is unique to *Neotroglia*, and is observed in
10
11
12 198 both species (Fig. 3C).

13
14 199 The gynosome is composed of the apical sclerite, spiny membrane and basal shaft
15
16
17 200 (Cheng et al., 2023). The gynosome is entirely placed anteriorly to the gonapophyses
18
19
20 201 in the noncopulating state (Fig. 2A). During copulation, all parts other than the basal
21
22
23 202 shaft protrude from the opening between the paraproct and gonapophyses (Fig. 1C, D).

24
25 203 There are six groups of muscles (dosp01, exsp01, spIX01, spIX02, gyIX01, gy-01; Fig.
26
27
28 204 2 E, G) connected to the gynosome, and four groups of those muscles are homologous
29
30
31 205 with those associated with the spermapore plates of other psocodeans (Cheng &
32
33
34 206 Yoshizawa, 2022). The gyIX01 (=M5 of Cheng et al., 2023) and gy-01 (= M6 of Cheng
35
36
37 207 et al., 2023) muscles are unique to *Sensitibillini*.

38
39 208

40 41 42 209 **Skeletal and muscle structures of male terminalia**

43
44 210 Among the male terminal structures, no obvious specificity was detected for the
45
46
47 211 clunium and epiproct. On the ventral side of each paraproct, a ridge is present, which
48
49
50 212 is triangular in the lateral view (Fig. 4A, C). Hook-like protrusions are also observed
51
52
53 213 on the paraproct of some other species of Psocodea but are generally located at the
54
55
56 214 posterior end of the paraproct (Yoshizawa, 2005). One group of muscles is associated
57
58
59 215 with the epiproct (epX01; Fig. 5C), and six groups of muscles with the paraproct

1 216 (paX01-04, papa01, pahy01; Fig. 5C). Among the latter, five groups of muscles
2
3 217 originate from the clunium, and one group of muscles originates from and inserts within
4
5
6 218 the paraproct (Fig. 5C). Since the epiproct, paraproct and clunium are present in both
7
8
9 219 sexes and have similar functions, five groups of muscles (epX01, paX01-04) can be
10
11 220 homologized between sexes (Fig. 5C and 8B; Cheng & Yoshizawa, 2022). The
12
13
14 221 following two groups of muscles are unique to males.
15

16
17 222 The hypandrium represents sternum IX and articulates laterally with the clunium.
18
19
20 223 The hypandrium has no obvious protrusions in *Neotroglia* (Fig. 4A, C). One group of
21
22
23 224 muscles is connected to the hypandrium (hyVIII01; Figs. 5E), which is homologous to
24
25
26 225 that observed in *Trichadenotecnum* (Fig. 3D).
27

28
29 226 The phallosome consists of two parts: a membranous pouch and a reversed U-
30
31 227 shaped thin sclerite surrounding the posterodorsal margin of the entrance of the
32
33
34 228 membranous pouch (Figs. 3F, G, 4E and 5A), which is only observed in *Neotroglia*
35
36
37 229 species. The phallosome closely fits into the concavity formed by the hypandrium in a
38
39
40 230 noncopulating state (Fig. 4E). During copulation, the sclerotized part of the phallosome
41
42
43 231 is raised upwards, and its apex rests on the protrusions of the paraproctal ridges (Fig.
44
45
46 232 4F). There are three groups of muscles (phIX01-02, phVIII01; Figs. 3F-I and 5G, H)
47
48
49 233 connected to the phallosome. Among them, phIX01 and phIX02 were also observed in
50
51 234 *Trichadenotecnum* (Fig. 3E).
52

53 235 **Male–female genital interaction**

54
55
56 236 In the copulating state, the male paraproct and epiproct are partly retracted inwardly.
57
58
59 237 The ventral paraproctal ridges, which are separated in the noncopulated condition, are
60
61
62
63
64
65

1 238 closely associated during copulation, together forming a single projection (Fig. 4A-D).
2
3 239 The sclerite of the phallosome protrudes upwards, and its apex fits with the anterior
4
5
6 240 margin of the male paraproctal projection (Fig. 4E, F). During copulation, these two
7
8
9 241 male structures securely sandwich the female dorsal valve from both sides (Fig. 6B:
10
11
12 242 blue arrow and Fig. 7: black dotted arrows).

13
14 243 The male genital cavity formed by the hypandrium and phallosome is opened and
15
16
17 244 exposed in the copulating condition (Fig. 4B, D). During copulation, the gynosome,
18
19
20 245 with the exception of the basal shaft, extends into the male's genital cavity. The apical
21
22
23 246 sclerite of the gynosome deeply penetrates the membranous pouch of the phallosome
24
25
26 247 (Fig. 6B: red arrow and Fig. 7). The spiny membrane of the gynosome expands to form
27
28
29 248 an internal anchor within the male genital cavity. The female epiproct and paraproct are
30
31
32 249 slightly retracted inwards. The concave ventral surface of the female paraproct and the
33
34
35 250 swollen gynosomal spiny area together anchor the male by sandwiching the
36
37
38 251 hypandrium externally (paraproct) and internally (gynosomal spines) (Fig. 6B: white
39
40
41 252 arrow and Fig. 7: red dotted arrows). The female external valves are opened and grasp
42
43
44 253 the lateral sides of the hypandrium (Figs 1F, 6A and 7).

45 254

47 255 **Discussion**

50 256 **Copulation process and holding mechanisms**

52
53 257 The present observation revealed that the following holding/locking systems are at
54
55
56 258 work during copulation to stabilize the coupling condition: (1) the female dorsal valve
57
58
59 259 is tightly sandwiched by the male paraproctal ridges and the tip of the phallosomal

1
2
3
4
5
6
7
8
9
10
11
12
13
14
15
16
17
18
19
20
21
22
23
24
25
26
27
28
29
30
31
32
33
34
35
36
37
38
39
40
41
42
43
44
45
46
47
48
49
50
51
52
53
54
55
56
57
58
59
60
61
62
63
64
65

1 260 sclerite; (2) the gynosomal spiny membrane anchors male internally by its inflation
2
3 261 within the male genital cavity; (3) the female paraproctal ventral concavities support
4
5
6 262 the ventral surface of the male hypandrium, and the hypandrium is sandwiched by the
7
8
9 263 female paraproct (ventrally) and the gynosomal spines (dorsally); and (4) the female
10
11
12 264 external valves grasp the lateral side of the male abdominal tip.

13
14 **265 Fixation of the female dorsal valve by the male**

15
16
17 266 During copulation, the female dorsal valve is almost fully inserted into the male and is
18
19
20 267 tightly held by the male's structures (the paraproctal ridges and the tip of the
21
22
23 268 phallosome sclerite; Figs 6B, red arrow and 7). In the copulating state, dosp01
24
25
26 269 connected to the female dorsal valve is in a relaxed state (Fig. 2F). Therefore, it is
27
28
29 270 assumed that this muscle is related to the re-storage of the dorsal valve at the end of
30
31
32 271 copulation. No muscle related to the protrusion of the dorsal valve were found.

33
34 272 Contractions of the male epiproctal and paraproctal muscles (epX01, paX01,
35
36 273 paX02, paX03, and pahy01) guide the male epiproct and paraproct to partly retract
37
38
39 274 inwardly (Figs 4C, D and 5D). The paired male paraproctal ridges are tightly associated
40
41
42 275 during copulation, together forming a single process, due to the contraction of paX03
43
44
45 276 (Figs 4B, D and 5D). In the meantime, the contraction of the phVIII01 muscle pulls the
46
47
48 277 phallosome upwards towards the paraproct (Figs 3I and 5H). The phIX01 muscle may
49
50
51 278 also have the function of protruding the phallosome. The merged male paraproctal
52
53
54 279 ridges buckle the ventral ridge of the female dorsal valve, and the other side of the
55
56
57 280 female dorsal valve is supported by the tip of the phallosomal sclerite (Figs 6B, blue
58
59 281 arrow and 7, black dotted arrows). Furthermore, the contraction of the pahy01 muscle

1 282 provides strong power to securely make the paraproct hooking and pulling the female
2
3 283 dorsal valve inward. The phIX01 and phIX02 muscles may also produce additional
4
5
6 284 power to move the apex of the phallosome inwards (i.e., pull the female dorsal valve
7
8
9 285 inwards, Fig. 1E). This clearly shows that the male *Neotroglia* actively holds the female
10
11
12 286 during copulation.

13
14 287 Similar movement of the phallosome to hold and fix the female genital structure
15
16
17 288 is also known in *Trichadenotecnum* (Psocomorpha: Psocidae: Cheng & Yoshizawa,
18
19
20 289 2019). However, in the case of *Trichadenotecnum*, the male holds the subgenital plate,
21
22
23 290 not the dorsal valve. In addition, the phIX01 and phIX02 muscles function to restore
24
25
26 291 the phallosome, and the phVIII01 muscle is absent in *Trichadenotecnum*. Therefore,
27
28
29 292 the female holding mechanism is apparently non-homologous between *Neotroglia* and
30
31 293 *Trichadenotecnum*.

32
33
34 294 At the end of the copulation, the paX01 and 02 muscles of the males are likely
35
36
37 295 contracted to move the paraproct outwardly, and phIX01 is contracted to restore the
38
39
40 296 phallosome. Both movements (active movements by the male) can function to release
41
42
43 297 the grasp on the female dorsal valve.

44 298 **Penetration of the gynosome and anchoring of the male**

45
46
47 299 To open the male genital cavity is very likely a prerequisite for the insertion of the
48
49
50 300 gynosome by a female. This is probably caused by two factors: 1) retraction of the male
51
52
53 301 paraprocts (see above), which are located above the genital chamber under
54
55
56 302 noncopulating conditions, thus blocking the male genital opening, and 2) backwards
57
58
59 303 movement of the posterior margin of the hypandrium. There is no muscle that causes
60
61
62
63
64
65

1 304 direct backwards movement of the posterior margin of the hypandrium. However, as
2
3 305 seen from Fig. 4B, the male terminalia are strongly compressed laterally during
4
5
6 306 copulation, which is very likely to cause the indirect backwards movement of the
7
8
9 307 posterior margin of the hypandrium (such as the mouth of a spring-loaded coin purse).
10
11 308 From the reconstructed 3D model of the copulating condition, two factors can be
12
13
14 309 assumed to be associated with the lateral compression of the male terminalia: 1)
15
16
17 310 contraction of the pahy01, phIX01 and 02 muscles causes the inward movement of the
18
19
20 311 lateral side of the hypandrium (i.e., male active movement); 2) grasping by the female
21
22
23 312 external valves causes compression force of the male terminalia (i.e., passive movement
24
25
26 313 for the male: see below).

27
28 314 The phIX01 and phIX02 muscles share the same origin on the hypandrium,
29
30
31 315 together forming a triangular configuration with the sclerite of the phallosome (Fig. 3H,
32
33
34 316 I). This state allows the hypandrium to move more effortlessly because the forces
35
36
37 317 generated by the two muscles are in the same plane. If the insertion site of these two
38
39
40 318 muscles on the hypandrium is not consistent, it is difficult to ensure that all the forces
41
42
43 319 are on the same plane, which will easily lead to conflicting forces. A similar
44
45
46 320 arrangement of the muscles has also been observed in the female external valves
47
48
49 321 (exIV01 and exIV02) of other psocodeans, such as *Lepinotus* and Amphientomidae,
50
51
52 322 which is also considered to cause effective movements of the valve (Cheng &
53
54
55 323 Yoshizawa, 2022).

56 324 Regarding the muscles attached to the gynosome, gy-01 relaxes and gyIX01
57
58
59 325 contracts in the copulating condition, and the status of these two muscles vice versa in
60
61
62
63
64
65

1 326 the non-copulating condition. Therefore, the contraction of gyIX01 apparently has a
2
3 327 function to extend the gynosome, and gy-01 works to restore the stuck gynosome to the
4
5
6 328 resting position (Fig. 2G, H). Two stout muscles, spIX01 and spIX02, relax during
7
8
9 329 copulation, thus restoring the gynosome membrane to its original shape and position
10
11 330 (Fig. 2G, H). The apical sclerite of the gynosome deeply penetrates the membranous
12
13
14 331 pouch of the phallosome during copulation, from which the semen is transported to the
15
16
17 332 female (Yoshizawa et al., 2014). The spiny membrane of the gynosome also enters the
18
19
20 333 male genital cavity (Figs. 1C, D, 6B and 7). Because no muscle is involved in inflating
21
22
23 334 the spiny membrane, the anchoring function of this specialized membrane is likely
24
25
26 335 achieved by increased body pressure. See also the next section for the additional
27
28
29 336 holding function of the gynosomal spines.

30
31 337 At the end of copulation, reduction of the internal pressure can cause the deflation
32
33
34 338 of the spiny membrane, and the contraction of the spIX01 and 02 muscles acts to restore
35
36
37 339 the gynosomal spiny membrane. The gynosome is retracted by the contraction of the
38
39
40 340 gy-01 muscle.

41 42 341 **Ventral fixation of the hypandrium**

43
44 342 The female paX01 and paX02 muscles are contracted during copulation, causing the
45
46
47 343 paraproct to be slightly indented in the direction of the female epiproct (Fig. 2D). The
48
49
50 344 female paX03 muscle retracts during copulation, directing the protrusions on the ventral
51
52
53 345 surface of the female paraproct inward (Figs. 1D and 2D). By this movement, the
54
55
56 346 ventrolateral paraproctal concavities form a continuous single circular concavity, which
57
58
59 347 fits perfectly to the curve of the ventral margin of the hypandrium (Fig. 6B, white
60
61
62
63
64
65

1 348 arrow).

2
3 349 The jointed female paraproctal cavities support the ventral surface of the male
4
5
6 350 hypandrium externally during copulation, which sandwich the hypandrium together
7
8
9 351 with the gynosomal spiny anchor within the male genital chamber (Figs. 6B, white
10
11
12 352 arrow and 7). Therefore, it is apparent that the female actively holds the male during
13
14
15 353 copulation by using the female paraproct and gynosome. Such close contact between
16
17 354 the female paraproct and the male hypandrium is not observed in *Trichadenotecnum*
18
19
20 355 (Cheng & Yoshizawa, 2019).

21
22
23 356 At the end of copulation, paX01 and 02 are probably contracted to release the
24
25
26 357 ventral paraproctal support of the male hypandrium.

27 28 358 **Grasping the male abdomen by the female external valves**

29
30
31 359 The exIX02 muscle is contracted during copulation and thus is associated with the
32
33
34 360 active opening of the female external valve at the beginning of copulation (Fig. 1C, F).

35
36 361 The female external valves grasp the lateral surface of the male hypandrium with
37
38
39 362 the contraction of the stout doex01 and exVIII01 muscles (Figs. 2E, F, 6A and 7). As
40
41
42 363 also mentioned above, this probably comprises two functions: opening the male genital
43
44
45 364 cavity at the beginning of copulation and holding the male during copulation, both of
46
47
48 365 which are active movements of the female.

49
50 366 At the end of copulation, exIX02 is probably contracted to open the external valves
51
52
53 367 to release the grasp on the male.

54
55
56 368 The functions of the muscles related to the external valve (opening/closing the
57
58
59 369 external valves) are also common in *Trichadenotecnum*. However, the external valve
60
61
62
63
64
65

1 370 of *Trichadenotecnum* does not have a function to grasp the male, and its closure muscles
2
3 371 hold the female subgenital plate, possibly to resist coercive mating by males (Cheng &
4
5
6 372 Yoshizawa, 2019).
7

8
9 **373 Sexual selection**

10
11 374 In animals with conventional sex roles, females usually gain fewer fitness benefits from
12
13
14 375 multiple matings, and thus, males more actively seek mating opportunities (Trivers,
15
16
17 376 1972). Accordingly, male animals sometimes develop elaborate genital structures for
18
19
20 377 coercive copulation with unwilling mates (Arnqvist & Rowe, 2002; Lange et al., 2013).
21
22
23 378 As counteradaptations, two types of traits are known to occur in female genitals:
24
25 379 “resistance” traits that decrease the male fitness component (e.g., efficiency of mate
26
27
28 380 holding) and “tolerance” traits that mitigate the costs of mating without affecting male
29
30
31 381 mating success (Reinhardt et al., 2014). In *Neotrogla*, males give nutritious seminal
32
33
34 382 gifts to females during copulation, which last up to 72 hours, and females mate multiply,
35
36
37 383 as is evident from the occurrence of multiple seminal capsules in the spermatheca
38
39 384 (Yoshizawa et al., 2014, 2018a). In addition, female *Neotrogla* possess twin
40
41
42 385 insemination slots with switching valves to receive double seminal gifts at the same
43
44
45 386 time (Yoshizawa et al., 2018a; Kamimura et al., 2021). Therefore, it has been assumed
46
47
48 387 in previous studies that female *Neotrogla* gain more net benefits from multiple
49
50
51 388 copulations than males and that females actively control copulatory processes by using
52
53 389 the unique intromittent organ (coupling-role reversal: Yoshizawa et al., 2014, 2019).

54
55
56 390 Our present study confirmed this view by showing that the multiple female organs
57
58 391 actively (and probably partly coercively) hold the male mate: this is achieved by
59
60
61
62
63
64
65

1 392 anchoring within the male genital chamber using the gynosomal spines and external
2
3 393 grasping using the female paraproct and the external valves. However, at the same time,
4
5
6 394 the 3D models also revealed that autonomous movements of male genital muscles are
7
8
9 395 necessary for the initiation of the copulatory processes and that male *Neotrogla* actively
10
11
12 396 hold the female mate during copulation.

13
14 397 The male paraproctal ridges and the tip of the phallosomal sclerite are tightly
15
16
17 398 associated even in the non-copulating condition in both *N. curvata* and *N. brasiliensis*
18
19
20 399 (Figs. 4A, C and 6C, D) and, without active upwards movement of the paraproct
21
22
23 400 (contraction of the paX01 and 02 muscles) of the male and downwards movement of
24
25
26 401 the phallosome (contraction of the phIX02 muscle), the female cannot insert the dorsal
27
28 402 valve into the genital cavity. To open the genital cavity is the most important
29
30
31 403 prerequisite for gynosomal insertion, and although its opening may partly be achieved
32
33
34 404 by the female's active movements (i.e., grasping of the terminalia using the external
35
36
37 405 valve), some male muscles (pahy01, phIX01 and phIX02) seem to be related to the
38
39 406 autonomous opening of the genital cavity. These male structures may also act to resist
40
41
42 407 coercive copulation by females.

43
44
45 408 In addition, the male securely fixes the female dorsal valve during copulation using
46
47
48 409 the male paraproctal ridges and the phallosomal sclerite. The well-developed male
49
50
51 410 muscles related to this fixation function, including some uniquely developed in
52
53 411 *Neotrogla*, strongly suggest that the secure holding of the mate during copulation is
54
55
56 412 also crucial for the male.

57
58
59 413 For some animals with conventional sex roles, mismatching in genital coupling is
60
61
62
63
64
65

1 414 known to result in leakage of seminal fluid, which can cause the female and male bodies
2
3 415 to stick together and thus reduce the rate of sperm transfer (Kamimura & Mistumoto,
4
5
6 416 2012; Tanaka et al., 2018; Polak & McEvey, 2022), or increasing the wounding
7
8
9 417 probability of the female genitals (Sota & Kubota, 1998; Kamimura, 2012; Masly &
10
11 418 Kamimura, 2014). In many of those cases, the females develop specific structures (such
12
13
14 419 as membranous pockets) that accommodate the wound-inflicting structures of the male
15
16
17 420 genitalia and thus mitigate the copulatory costs (Sota & Kubota, 1998; Kamimura,
18
19
20 421 2012). Interestingly, male *Neotroglia* possess species-specific pockets on the walls of
21
22
23 422 the genital chamber to receive gynosomal spines, although no copulatory wounds have
24
25
26 423 been detected there (Yoshizawa et al., 2014). Given that the copulatory mechanism of
27
28
29 424 *Neotroglia* is complicated, seminal fluid passed to the female is voluminous and
30
31
32 425 possibly reactive (Yoshizawa et al., 2014). Considering that the females' anchoring
33
34
35 426 power is very strong (an artificial trial to separate a coupled specimen led to separation
36
37
38 427 of the male abdomen from the thorax without breaking the genital coupling: Yoshizawa
39
40
41 428 et al., 2014), a precisely connected genital complex and step-by-step releases of each
42
43
44 429 holding mechanism achieved by the cooperation of both sexes are probably beneficial
45
46
47 430 for both males and females. Such concordance of the interests between the sexes may
48
49
50 431 have prompted the evolution of "tolerance" traits in male *Neotroglia*, as in a completely
51
52
53 432 sex-role reversed mating scenario.

54 433

55 434 **Conclusion**

56
57
58 435 Inverted genital couplings of *Neotroglia* provide an extremely rare opportunity to test
59
60
61
62
63
64
65

1 436 hypotheses on the evolution of genital structures (House & Simmons, 2006; Simmons,
2
3 437 2014; Michels et al., 2015) under the reversed direction of sexual selection. We found
4
5
6 438 evidence of the complicated coexistence of genital structures, suggesting male
7
8
9 439 resistance, female coercion, and cooperation between the sexes. The absence of harmful
10
11
12 440 structures that inflict wounds on the opposite sex in both males and females is notable.
13
14
15 441 The coevolution between the male and female genital structures in *Neotroglia* may
16
17
18 442 provide a new example for the evolution of tolerance traits, a newly proposed idea
19
20
21 443 concerning genital evolution (Michels et al., 2015).

22
23 444 For further understanding of the sexual selection and evolution of novelties,
24
25
26 445 detailed information of the courtship behaviour of *Neotroglia* and its relatives is key but
27
28
29 446 is very poorly understood to date. Accumulation of basic behavioural information is
30
31
32 447 highly desired for a more accurate and detailed understanding of the evolution of the
33
34
35 448 gynosome in *Neotroglia*.

36
37 449

40 450 **Acknowledgement**

41
42
43 451 We thank Kentaro Uesugi for support with the μ CT imaging. Research at Spring-
44
45
46 452 8 was approved through project numbers 2016A1269 (leader: Ryuichiro Machida),
47
48
49 453 2017B1712 and 2018B1725 (Naoki Ogawa). This work was supported by Japan
50
51
52 454 Society for the Promotion of Science, grant numbers 20J2088301 to ZC and 15H04409
53
54
55 455 and 19H03278 to KY. RLF thanks the Conselho Nacional de Desenvolvimento
56
57
58 456 Científico e Tecnológico (CNPq grant n. 308334/2018-3).

1 457

2
3
4
5 458 **Declarations**

6
7
8 459 **Conflict of Interest** The authors declare no conflict of interests

9
10
11 460

12
13
14 461 **References**

15
16 462 Arnqvist G, Rowe L (2002) Correlated evolution of male and female morphologies in
17 water striders. *Evolution* 56:936–947. [https://doi.org/10.1111/j.0014-](https://doi.org/10.1111/j.0014-3820.2002.tb01406.x)
18
19 463
20
21 464 3820.2002.tb01406.x

22
23
24 465 Cheng Z, Yoshizawa K (2019) Functional morphology of Trichadenotecnum male and
25 female genitalia analyzed using μ CT (Insecta: Psocodea: Psocomorpha). *J Morph* 280:
26 466 555-567. <https://doi.org/10.1002/jmor.20965>
27
28 467

29
30
31 468 Cheng Z, Yoshizawa K (2022) Exploration of the homology among the muscles
32 associated with the female genitalia of the three suborders of Psocodea
33 469 associated with the female genitalia of the three suborders of Psocodea
34 (Insecta). *Arthropod Str Dev* 66:101141. <https://doi.org/10.1016/j.asd.2022.101141>
35
36 470

37
38
39 471 Cheng Z, Kamimura Y, Ferreira RL, Lienhard C, Yoshizawa K (2023) Acquisition of
40 472 novel muscles enabled protruding and retracting mechanisms of female penis in sex-
41 role reversed cave insects. *Roy Soc Open Sci.* 10:220471. [10.1098/rsos.220471](https://doi.org/10.1098/rsos.220471)
42
43 473

44
45
46 474 Gwynne DT (2008) Sexual conflict over nuptial gifts in insects. *Ann Rev Entomol* 53:
47 83-101. [10.1146/annurev.ento.53.103106.093423](https://doi.org/10.1146/annurev.ento.53.103106.093423)
48
49 475

50
51
52 476 House CM, Simmons LW (2006) Offensive and defensive sperm competition roles in
53 the dung beetle *Onthophagus taurus* (Coleoptera: Scarabaeidae). *Behav Ecol Sociobiol*
54 477 60:131-136. <https://www.jstor.org/stable/25063796>
55
56 478

57
58
59
60 479 Kamimura Y (2012) Correlated evolutionary changes in *Drosophila* female genitalia
61
62
63
64
65

1 480 reduce the possible infection risk caused by male copulatory wounding. Behav Ecol
2 Sociobiol 66:1107-1114. 10.1007/s00265-012-1361-0
3
4
5
6 482 Kamimura Y, Mitsumoto H (2012) Lock- and- key structural isolation between sibling
7
8 483 *Drosophila* species. Entomol Sci 15:197-201. <https://doi.org/10.1111/j.1479->
9
10 484 8298.2011.00490.x
11
12
13 485 Kamimura Y, Yoshizawa K, Lienhard C, Ferreira RL, Abe J (2021) Evolution of nuptial
14
15 486 gifts and its coevolutionary dynamics with male-like persistence traits of females for
16
17 487 multiple mating. BMC Ecol Evol 21:164. <https://doi.org/10.1186/s12862-021-01901-x>
18
19
20
21 488 Klier E (1956) Zur Konstruktionsmorphologie des männlichen Geschlechtsapparates
22
23 489 der Psocopteren. Zool Jahr (Anat.) 75:207–286.
24
25
26 490 Lange R, Reinhardt K, Michiels NK, Anthes N (2013) Functions, diversity, and
27
28 491 evolution of traumatic mating. Biol Rev 88:585–601. 10.1111/brv.12018
29
30
31
32 492 Lewis S, South A (2012) The evolution of animal nuptial gifts. In *Advances in the Study*
33
34 493 *of Behavior* (Vol. 44, pp. 53-97). Academic Press. 10.1016/B978-0-12-394288-
35
36 494 3.00002-2
37
38
39 495 Lienhard C (1998) Psocoptères euro-méditerranéens. Faune France 83:1-517.
40
41
42
43 496 Lienhard C (2007) Description of a new African genus and a new tribe of
44
45 497 Speleketorinae (Psocodea: 'Psocoptera': Prionoglarididae). Rev suiss Zool 114:441-
46
47 498 469. 10.5962/bhl.part.80399
48
49
50
51 499 Lienhard C, Carmo TOD, Ferreira RL (2010) A new genus of Sensitibillini from
52
53 500 Brazilian caves (Psocodea: 'Psocoptera': Prionoglarididae) Rev Swiss Zool 117:611-635.
54
55 501 10.5962/bhl.part.117600
56
57
58 502 Lienhard C, Ferreira RL (2013) A new species of *Neotroglia* from Brazilian caves
59
60 503 (Psocodea:'Psocoptera': Prionoglarididae). Rev Swiss Zool 120:3-12.
61
62
63
64
65

1 504 Masly JP, Kamimura Y (2014) Asymmetric mismatch in strain-specific genital
2 morphology causes increased harm to *Drosophila* females. *Evolution* 68:2401-2411.
3
4 506 10.1111/evo.12436
5
6
7
8 507 Michels J, Gorb SN, Reinhardt K (2015) Reduction of female copulatory damage by
9 resilin represents evidence for tolerance in sexual conflict. *J Roy Soc*
10 508 *Interface* 12:20141107. 10.1098/rsif.2014.1107
11
12 509
13
14
15 510 Polak M, McEvey SF (2022) Refutation of traumatic insemination in the *Drosophila*
16 *bipunctinata* species complex. *Biol Lett* 18:20210625.
17 511 <https://doi.org/10.1098/rsbl.2021.0625>
18
19 512
20
21
22
23 513 Simmons LW (2014). Sexual selection and genital evolution. *Austral Entomol* 53:1-
24
25 514 17. <https://doi.org/10.1111/aen.12053>
26
27
28
29 515 Sota T, Kubota K (1998) Genital lock- and- key as a selective agent against
30 hybridization. *Evolution* 52:1507-1513. 10.1111/j.1558-5646.1998.tb02033.x
31 516
32
33
34
35 517 Tanaka KM, Kamimura Y, Takahashi A (2018) Mechanical incompatibility caused by
36 modifications of multiple male genital structures using genomic introgression in
37 518 *Drosophila*. *Evolution* 72:2406-2418. 10.1111/evo.13592
38
39 519
40
41
42
43 520 Trivers RL (1972). Parental investment and sexual selection. In *Sexual Selection and*
44 521 *the Descent of Man, 1871–1971*. Aldine Publishing.
45
46
47
48
49 522 Uesugi K, Hoshino M, Takeuchi A, Suzuki Y, Yagi N (2012) Development of fast and
50 523 high throughput tomography using CMOS image detector at SPring-8. *Dev X-Ray*
51
52 524 Tomography VIII 8506:85060I. 10.1117/12.929575
53
54
55
56
57
58 525 Uesugi K, Hoshino M, Takeuchi A (2017) Introducing high efficiency image detector
59
60
61
62
63
64
65

1 526 to X-ray imaging tomography. J Phys Conference Series 849:012051. 10.1088/1742-
2
3 527 6596/849/1/012051
4
5
6
7 528 Yoshizawa K (2001) A systematic revision of Japanese *Trichadenotecnum* Enderlein
8
9 529 (Psocodea:'Psocoptera': Psocidae: Ptyctini), with redefinition and subdivision of the
10
11 530 genus. Invertebr Syst 15:159–204. 10.1071/IT00013
12
13
14 531 Yoshizawa K (2005) Morphology of Psocomorpha (Psocodea:' Psocoptera'). Insecta
15
16 532 Matsumurana NS 62:1–44.
17
18
19
20 533 Yoshizawa K, Ferreira RL, Kamimura Y, Lienhard C (2014) Female penis, male vagina,
21
22 534 and their correlated evolution in a cave insect. Curr Biol 24:1006-1010.
23
24 535 <https://doi.org/10.1016/j.cub.2014.03.022>
25
26
27
28 536 Yoshizawa K, Kamimura Y, Lienhard C, Ferreira RL, Blanke A (2018a) A biological
29
30 537 switching valve evolved in the female of a sex-role reversed cave insect to receive
31
32 538 multiple seminal packages. eLife 7:e39563. 10.7554/eLife.39563.
33
34
35 539 Yoshizawa K, Ferreira RL, Yao I, Lienhard C, Kamimura Y (2018b) Independent
36
37 540 origins of female penis and its coevolution with male vagina in cave insects (Psocodea:
38
39 541 Prionoglarididae). Biol Lett 14:20180533. <https://doi.org/10.1098/rsbl.2018.0533>
40
41
42
43 542 Yoshizawa K, Ferreira RL, Lienhard C, Kamimura Y (2019) Why did a female penis
44
45 543 evolve in a small group of cave insects?. BioEssays 41:1900005.
46
47 544 10.1002/bies.201900005
48
49
50
51 545 Yushkevich PA, Piven J, Hazlett HC, Smith RG, Ho S, Gee JC, Gerig G (2006) User-
52
53 546 guided 3D active contour segmentation of anatomical structures: significantly
54
55
56 547 improved efficiency and reliability. Neuroimage 31:1116-1128.
57
58
59 548 <https://doi.org/10.1016/j.neuroimage.2006.01.015>
60
61
62
63
64
65

1 549 **Figure Legends**

2
3 550 **Fig. 1.** 3D reconstruction of the female terminalia of *Neotroglia curvata*; (for E-G left:
4
5
6 551 noncopulating state; right: copulating state): (A) ventral view, noncopulating state; (B)
7
8
9 552 posterior view, noncopulating state; (C) ventral view, copulating state; (D) posterior
10
11
12 553 view, copulating state; (E) lateral view (highlighting dorsal valve); (F) lateral view
13
14 554 (highlighting the external valve); (G) lateral view (highlighting the gynosome).
15
16
17 555 Abbreviations: ep = epiproct; pa = paraproct; cl = clunium; st = sternum; gy =
18
19
20 556 gynosome; do = dorsal valve; ex = external valve.
21

22 557 **Fig. 2.** 3D reconstruction of the female terminalia of *Neotroglia curvata*, internal view;
23
24
25 558 noncopulating state (A, C, E and G); copulating state (B, D, F, and H); highlighting
26
27
28 559 different structures and associated muscles (C-H): (1) epX01; (2) paX01; (3) paX02;
29
30
31 560 (4) paX03; (5) paX04; (6) dosp01; (7) doex01; (8) exsp01; (9) exIX02; (10) exVIII01;
32
33
34 561 (11) spIX01; (12) spIX02; (13) gygy01; (14) gy-01. See Fig. 1 for abbreviations.
35

36 562

37
38
39
40 563 **Fig. 3.** 3D reconstruction of the terminalia in the noncopulating state (A-H) and
41
42
43 564 copulating state (I), highlighting different structures and associated muscles: female
44
45
46 565 *Neotroglia curvata* (A,B); female *N. brasiliensis* (C); male *Trichadenotecnum*
47
48
49 566 *pseudomedium* (D,E); male *N. brasiliensis* (F,G); male *N. curvata* (H,I). (A-C) Ventral
50
51
52 567 view; (D-F) internal view; (G-I) lateral view. Abbreviations: ep = epiproct; pa =
53
54 568 paraproct; hy = hypandrium; cl = clunium; ph = phallosome.
55
56

57 569

58
59
60 570 **Fig. 4.** 3D reconstruction of the male terminalia of *Neotroglia curvata*, noncopulating
61
62
63
64
65

1 571 state (A, C and E); copulating state (B, D and F): (A, B) posterior view; (C, D) lateral
2
3 572 view; (E, F) lateral view (highlighting the phallosome). Abbreviations: sg = segment
4
5
6 573 VIII; m= membrane; for others, see Fig. 3.

7
8
9 574 **Fig. 5.** 3D reconstruction of the male terminalia of *Neotroglia curvata*, internal view;
10
11 575 noncopulating state (A, C, E and G); copulating state (B, D, F and H), highlighting
12
13 576 different structures and associated muscles (D-H): (1) epX01; (2) paX01; (3) paX02;
14
15 577 (4) paX03; (5) paX04; (6) pahy01; (7) papa01; (8) hyVIII01; (9) phIX01; (10) phIX02;
16
17 578 (11) phVIII01. Abbreviations: te = tergum; m= membrane; for others, see Fig. 3.

18
19
20 579 **Fig. 6.** *Neotroglia curvata*, 3D reconstruction of terminalia of the copulating pair, lateral
21
22 580 view (A,B); *N. brasiliensis*, 3D reconstruction of terminalia of the male in the
23
24 581 noncopulating state (C,D). (B) highlighting the gynosome, phallosome, paraproct (m)
25
26 582 and epiproct (m); (C) posterior view; (D) lateral view, highlighting the phallosome and
27
28 583 paraproct (m). See Figs. 1 and 3 for abbreviations.

29
30
31 584 **Fig. 7.** Schematic drawing of the male and female genitalia of *Neotroglia curvata*
32
33 585 in copulated condition. Gray indicates male structures, and orange indicates female
34
35 586 ones. Black arrows indicate holding system by male, and red arrows indicate that by
36
37 587 female.

38
39
40 588 **Fig.8.** *Neotroglia curvata* in an uncopulated state, putative groundplan configuration of
41
42 589 the terminalia (internal view), schematic (based on the 3D reconstruction of the *N.*
43
44 590 *curvata*). (a) female; (b) male. Lines indicate muscles. Except for muscle paX04, all
45
46 591 dotted lines indicate the muscles attached to the gynosome membrane. (1) epX01; (2)
47
48 592 paX01; (3) paX02; (4) paX03; (5) paX04; (6) dosp01; (7) doex01; (8) exsp01; (9)

1 593 exIX02; (10) exVIII01; (11) spIX01; (12) spIX02; (13) gygy01; (14) gy-01; (15)
2
3 594 pahy01; (16) papa01; (17) hyVIII01; (18) phIX01; (19) phIX02; (20) phVIII01. See
4
5
6 595 Figs. 1 and 3 for abbreviations.
7
8
9 596

10
11
12
13
14
15
16
17
18
19
20
21
22
23
24
25
26
27
28
29
30
31
32
33
34
35
36
37
38
39
40
41
42
43
44
45
46
47
48
49
50
51
52
53
54
55
56
57
58
59
60
61
62
63
64
65

Figure 1

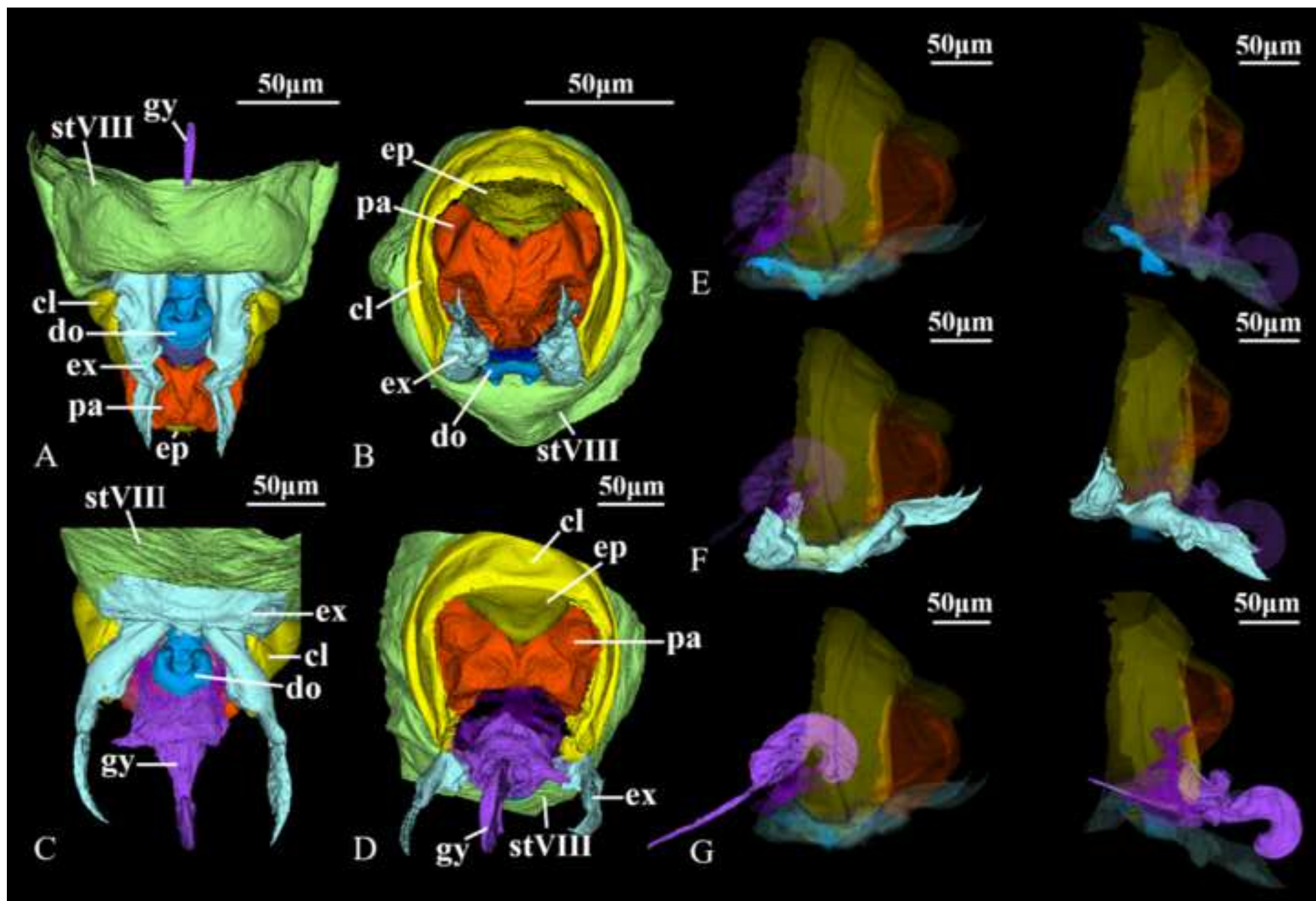


Figure 2

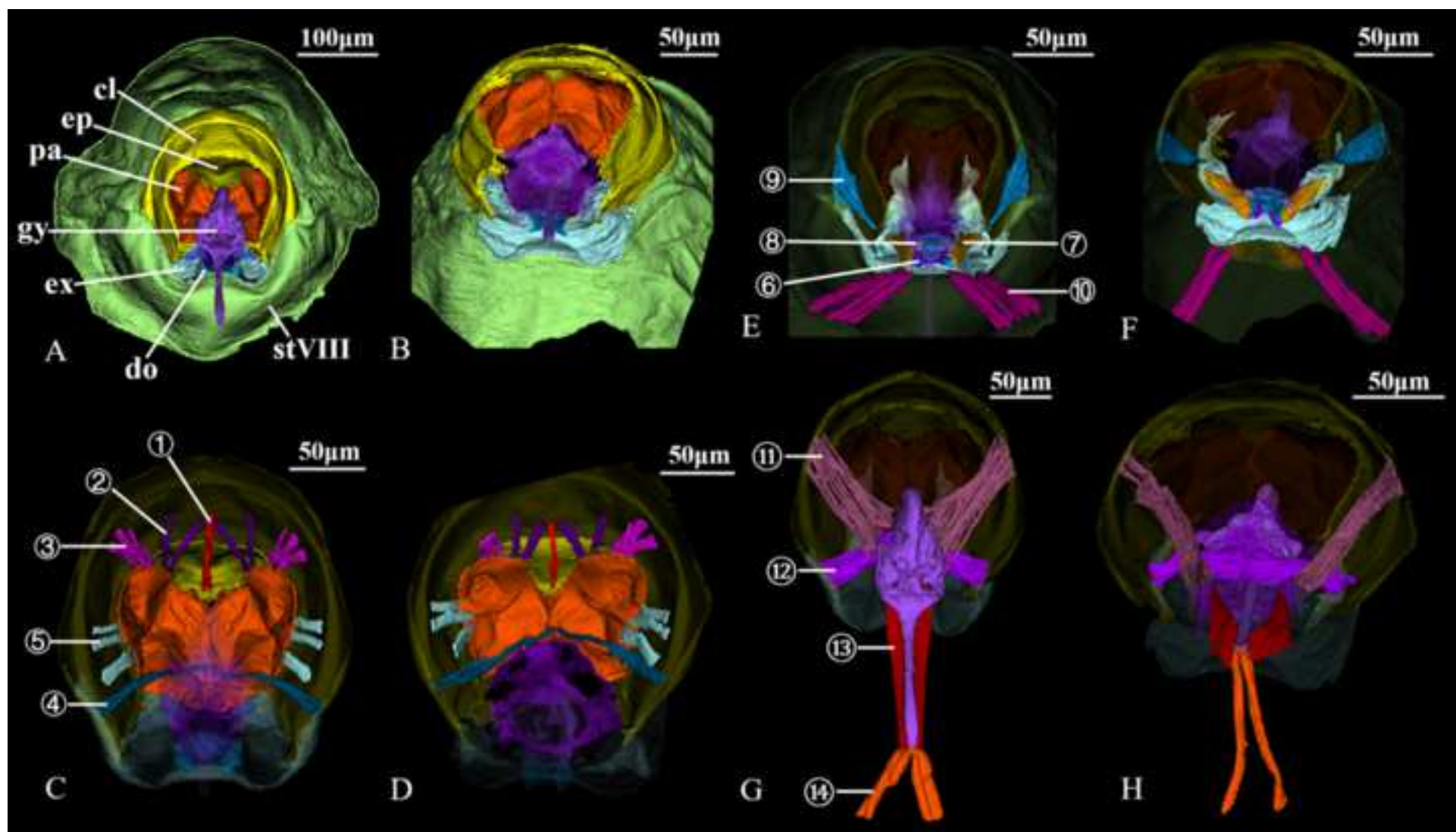


Figure 3

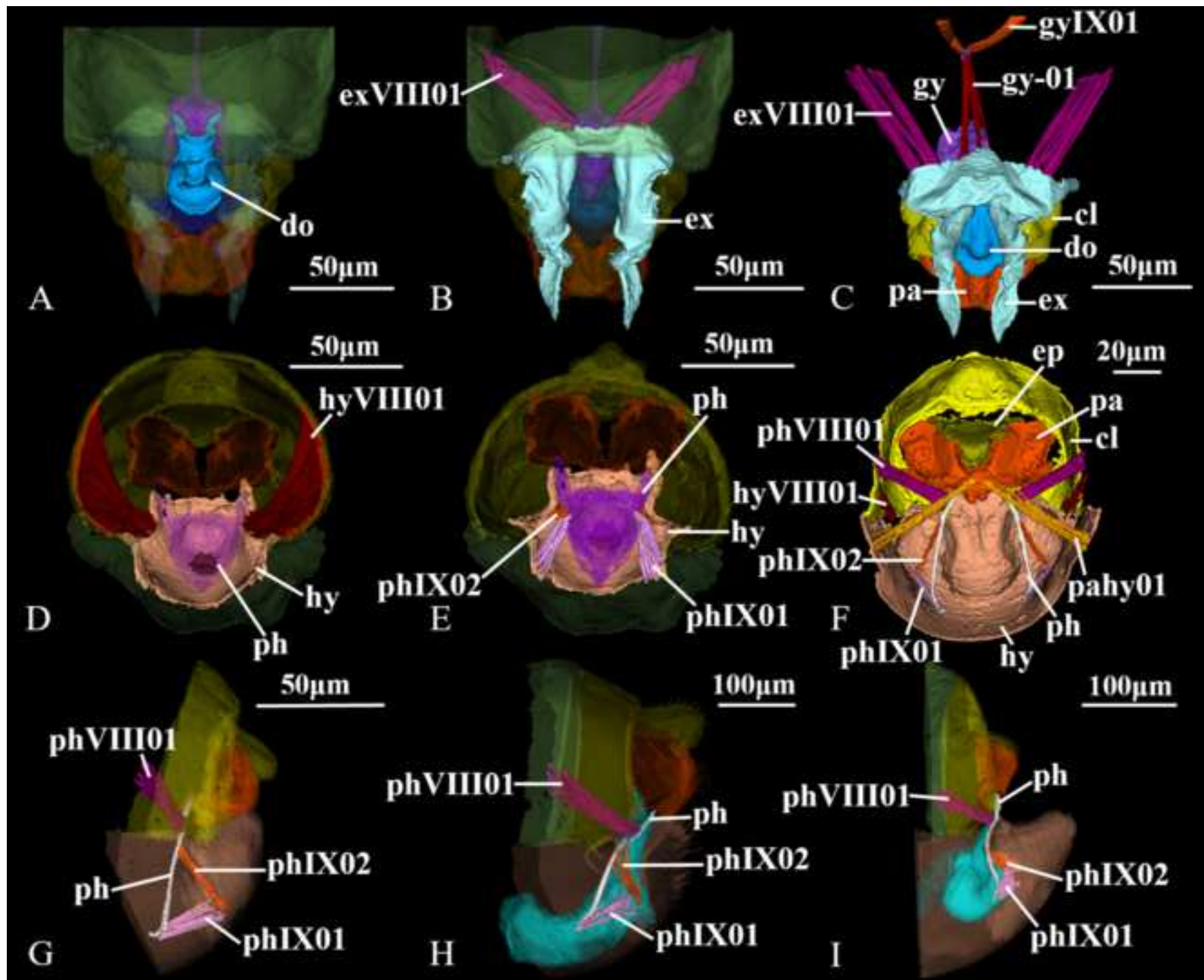


Figure 4

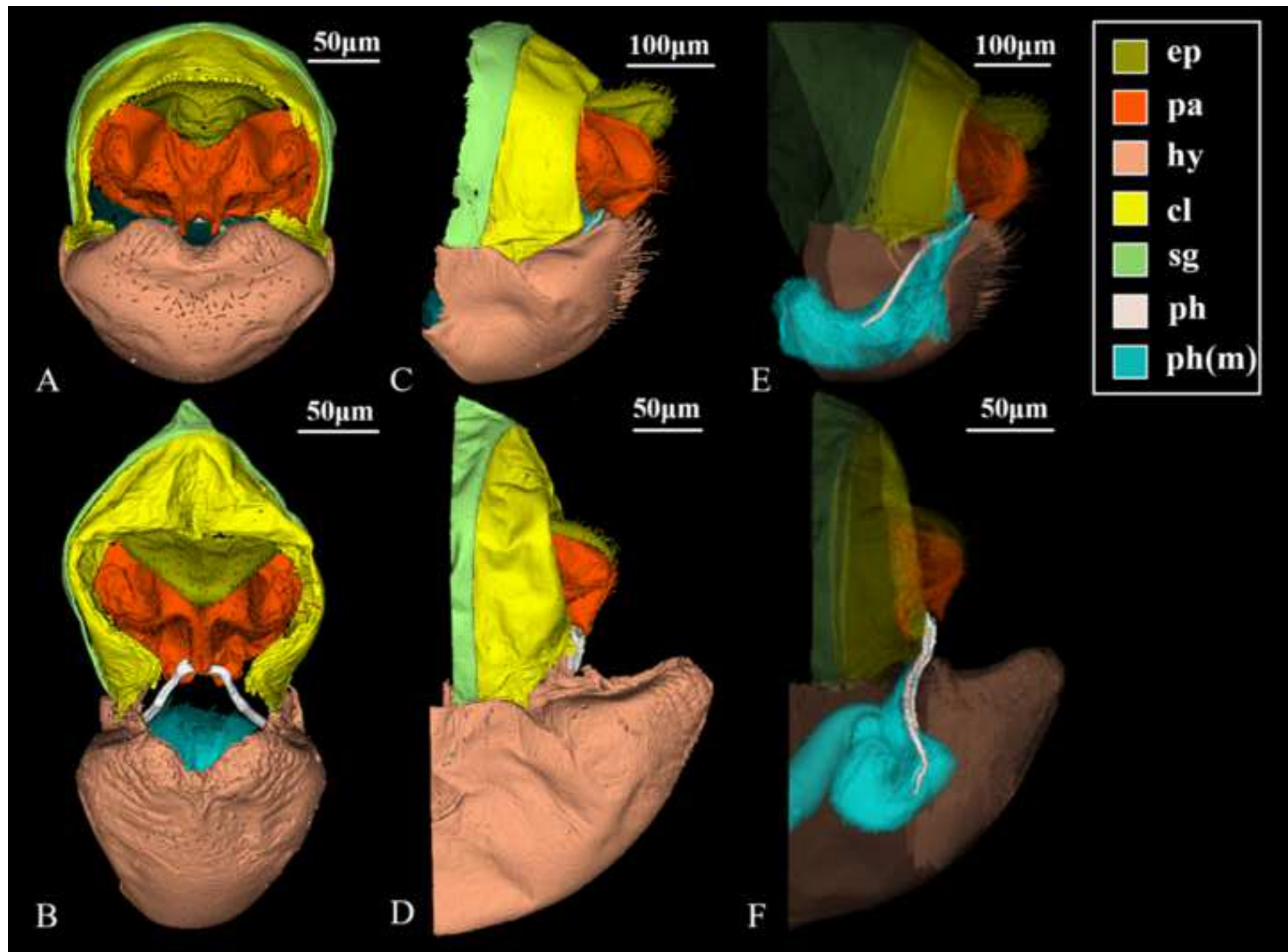


Figure 5

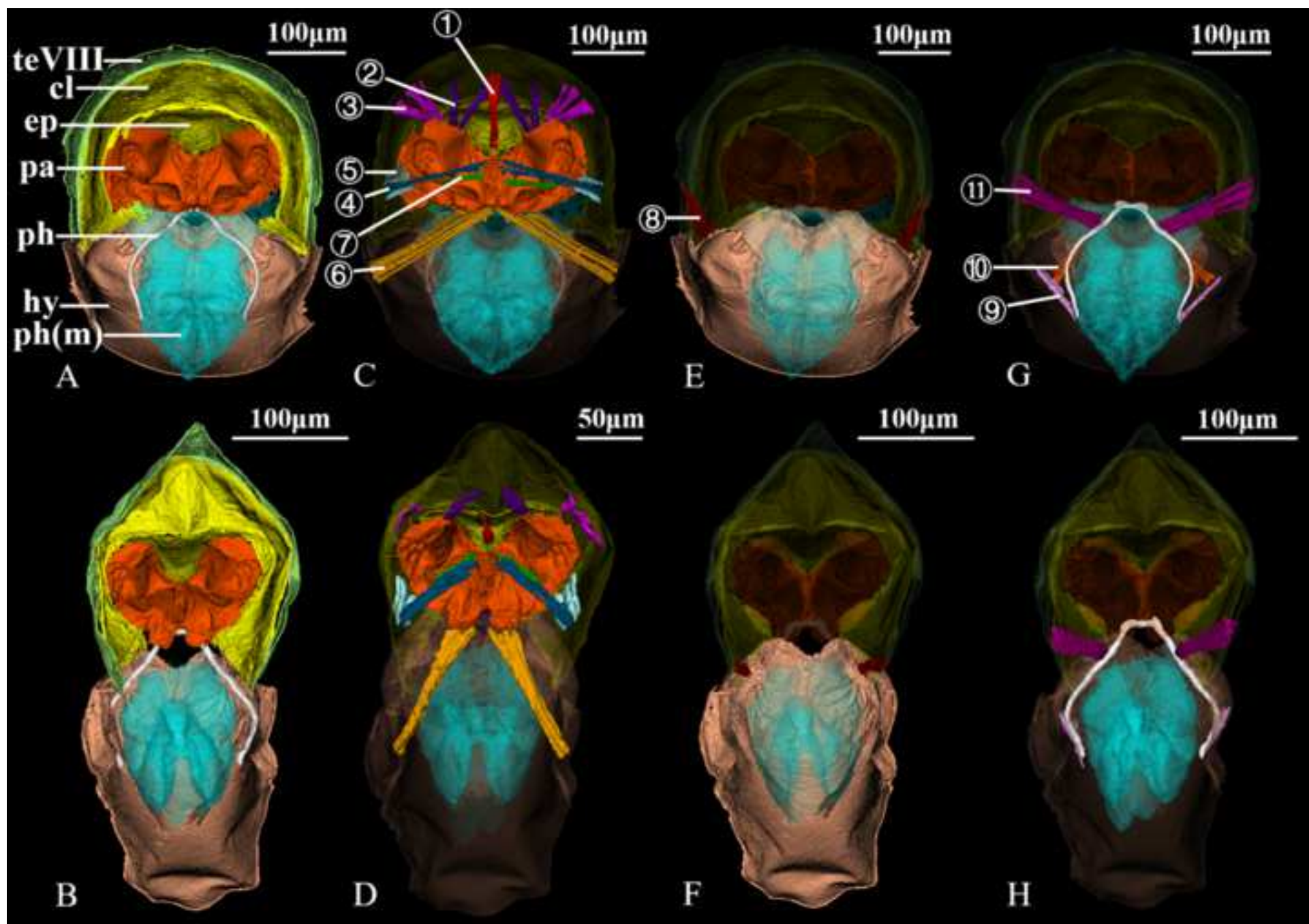


Figure 6

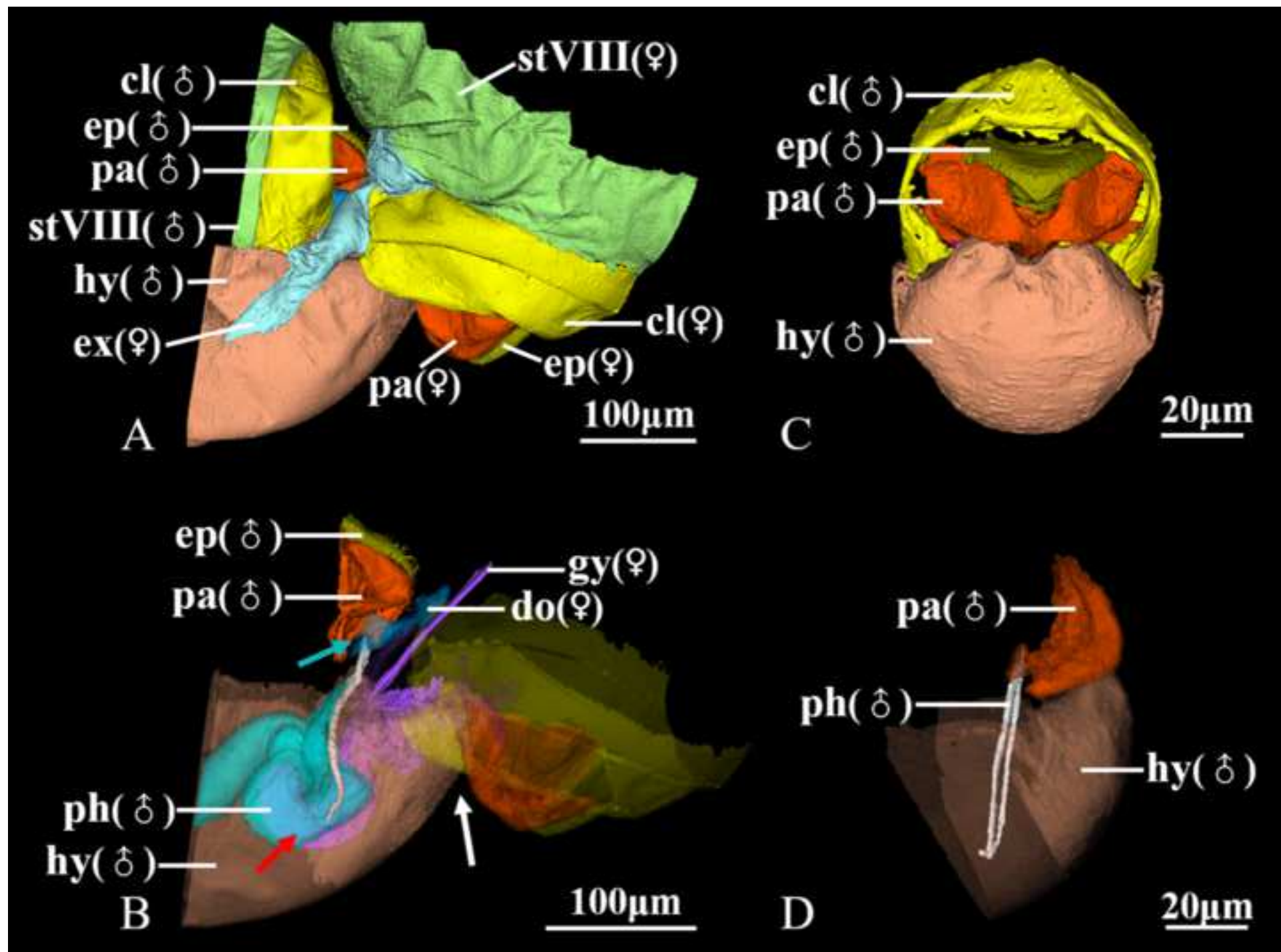


Figure 7

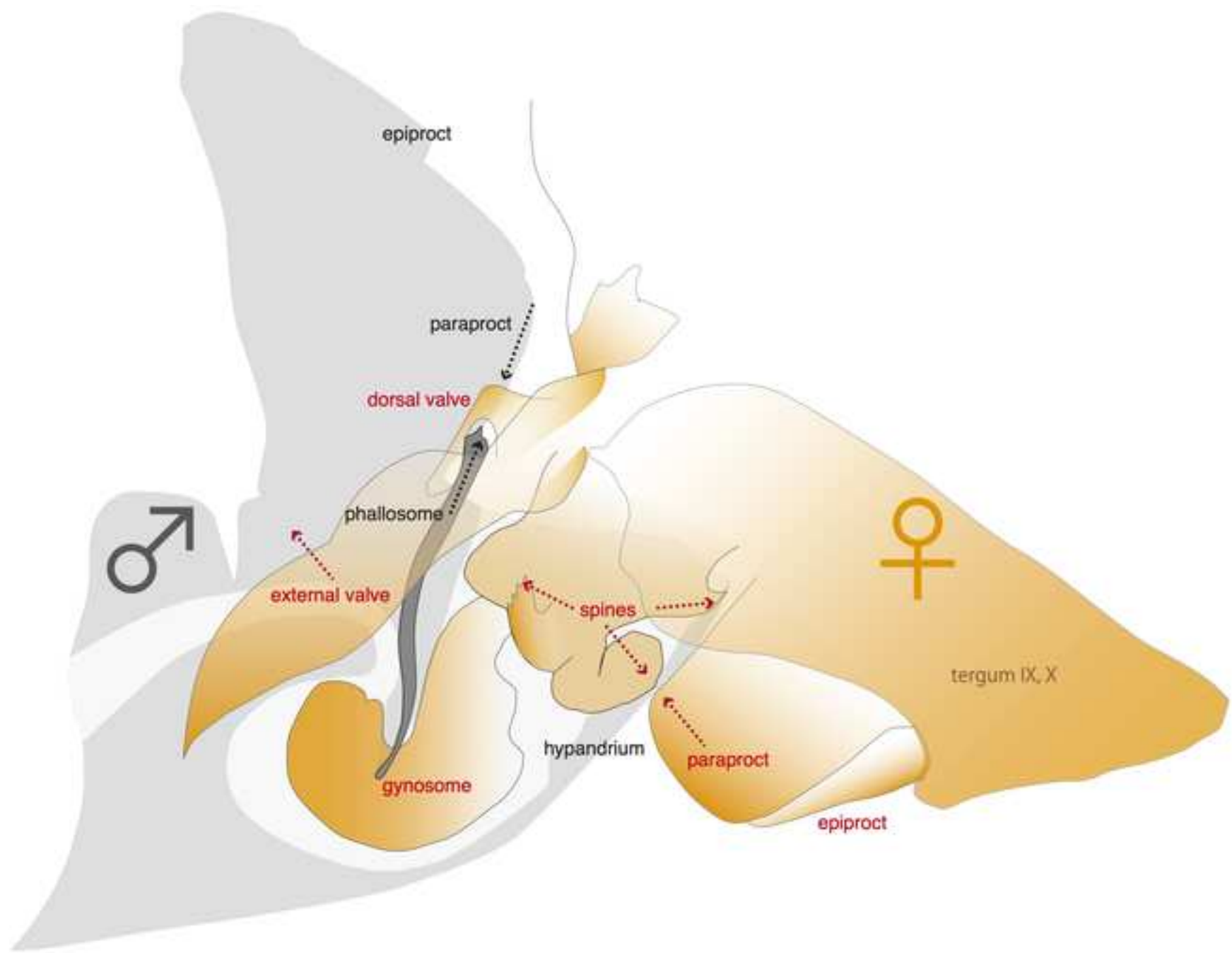


Figure 8

